PHYSICAL REVIEW E VOLUME 58, NUMBER 4 OCTOBER 1998

Differential flow induced chemical instability and Turing instability for Couette flow

Y. Balinsky (Khazan)
Programme in Applied Mathematics, Technion–Israel Institute of Technology, 32000 Haifa, Israel

L. M. Pismen
Department of Chemical Engineering and Minerva Center for Nonlinear Physics of Complex Systems,
Technion–Israel Institute of Technology, 32000 Haifa, Israel

(Received 2 March 1998)

Conditions of differential flow induced chemical instability (DIFICI) are obtained for heterogeneous reactions in a Couette flow reactor with diffusional supply of reactants. We describe a general method applicable to the analysis of a surface reaction fed by diffusion and laminar advection that reduces the original three-dimensional problem to a closed two-dimensional evolution equation containing a nonlocal Dirichlet to Neumann operator. This procedure is applied to compute conditions of DIFICI and competing symmetry-breaking instabilities for a bimolecular catalytic reaction and the Brusselator model. [S1063-651X(98)00310-9]

PACS number(s): 47.20.Ky, 82.65.Jv, 05.70.Ln

I. INTRODUCTION

A *differential flow* is a bulk flow in a mixture in which two or more components move with different velocities in the reaction region [1]. A differential flow between the counteracting species of dynamical activator-inhibitor system may destabilize its homogeneous reference state through the *differential flow induced chemical instability* (DIFICI). The DIFICI was predicted theoretically [2] in one spatial dimension and verified experimentally in the Belousov-Zhabotinsky system [3].

The primary role of diffusion in Turing instability is to spatially disengage the counteracting species. A standard system exhibiting Turing instability includes a slowly diffusing activator and a rapidly diffusing inhibitor [5]. The symmetry breaking occurs when the inhibitor diffusing away from active locations suppresses chemical activity in their neighborhood. Differential flow of activator and inhibitor can destabilize a spatially homogeneous state of the system similarly to differential diffusivity in the case of Turing instability. The homogeneous steady state may be destabilized when the activator and the inhibitor are advected at different flow rates, regardless of which one is faster, so that one is not constrained by the requirement of a higher diffusive rate of the inhibitor characteristic to the classical Turing mechanism.

The aim of our investigation is to establish DIFICI conditions for a realistic system where spatially homogeneous states exist (before being broken) in spite of a prevalently advective transport. A system of this kind cannot be one dimensional, as the reaction zone must be homogeneously accessible to mass transport. In a previous work [4] we have shown that DIFICI may indeed occur in an autocatalytic reaction on the equiaccessible surface of a *rotating disk*. Here we shall consider in more detail another suitable system: a heterogeneous chemical reaction on a *rotating cylinder*. The advantage of this case is a simple flow pattern and a possibility to follow a competition between the DIFICI and Turing symmetry-breaking mechanism. Differential flow near a cylinder, as well as near a disk, is possible due to different adsorption rates and surface capacitances of different reactants.

We consider Couette flow between two coaxial cylinders with radii r_0 and r_1 ($r_0 < r_1$), as shown in Fig. 1. The inner cylinder is at rest and serves as a catalytic surface, while the reactants are supplied from the outer cylinder that rotates with angular velocity ω (an alternative configuration with a stationary outer and rotating inner cylinder is equivalent). This system can be realized experimentally by making the outer surface porous or semipermeable.

The paper is organized as follows. In Sec. II we formulate a general problem of adsorption and reaction on an equiaccessible surface with reactants supplied and products removed by diffusion and advection and obtain an implicit stability condition dependent on a *transport operator* that relates the deviation of the external flux to deviations of concentrations. The spectrum of the transport operator is computed in Sec. III for Couette flow. In Secs. IV and V conditions of DIFICI and competing instabilities are computed for a bimolecular catalytic reaction and for the Brusselator model.

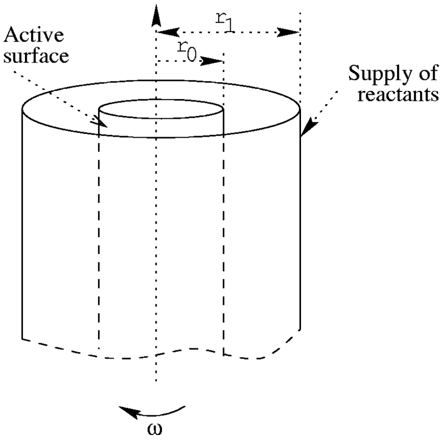

FIG. 1. Couette flow between two coaxial cylinders with radii r_0 and r_1 ($r_0 < r_1$). The inner cylinder is at rest and serves as a catalytic surface; the outer cylinder rotates with angular velocity ω.

II. SURFACE REACTION

A. Balance equations

We consider a catalytic reaction on the surface of a cylinder, assumed to be sufficiently large in the direction of the rotation axis, so that the edge effects are negligible. The reactants are advected by the ambient flow, assumed to be laminar. Equations on the surface include effects of adsorption and surface reaction

$$\gamma \frac{\partial \theta_j}{\partial t^*} = \mathcal{G}_j^* + R_j^* ,$$

where θ_j are surface concentrations for different species, γ is the adsorption capacity per unit area, R_j^* is the production rate of the jth reactant in surface reactions (dependent, generally, on concentrations of all adsorbed species), and $\mathcal{G}_j^*$ is the net adsorption rate. The net adsorption rates can be expressed through the diffusional flux at the catalytic surface

$$\mathcal{G}_j^* = \frac{D_j^*}{\chi} \left(\frac{\partial c_j^*}{\partial r^*} \right),$$

where χ is a geometric factor expressing the active surface area per unit nominal geometric area of the catalytic surface and r^* is the coordinate normal to the catalytic surface. Assuming adsorption equilibrium described by isotherms $\theta_j = \theta_j(\mathbf{c}^*)$ yields a relation between surface concentrations and bulk concentrations near the surface. Rescaling the reaction rate R_j^* by a reaction rate coefficient κ and time by the reaction time scale κ/γ we obtain the nondimensional equations on the catalytic surface

$$\mathbf{W} \frac{\partial \mathbf{c}}{\partial t} = \mathbf{P} \frac{\partial \mathbf{c}}{\partial r} + \mathbf{f}(\mathbf{c}), \tag{1}$$

where $c_j = c_j^*/C_j^*$ is the dimensionless bulk concentration near the catalytic surface and $r = r^*/l$ is the nondimensional coordinate. The scales C_j^* of the bulk concentrations and the length scale l should be specified later. The matrix $\mathbf{W}$ with elements $W_{jm} = \partial \theta_j / \partial c_m$ is defined by adsorption isotherms. $\mathbf{P}$ is a diagonal matrix with the elements $P_{jj} = D_j C_j^* / (\chi l \kappa) = d_j C_j / p$, where $d_j = D_j / D_1$ are rescaled diffusion coefficients and $p = \chi l \kappa / (D_1 C_1^*)$; $C_j = C_j^* / C_1^*$ is a scale ratio of bulk concentrations.

The diffusional flux $\mathcal{G}^*$ is represented by a *linear* Dirichlet to Neumann pseudodifferential operator $\partial \mathbf{c} / \partial r = \mathbf{G}(\mathbf{c})$. The linear operator $\mathbf{G}$ should be defined by solving the transport problem for the reactants supplied from the bulk.

B. Stationary states and stability

In a stationary state the transport rate can be expressed as $q_j^0 (c_j^e - c_j^s)$, where q_j^0 is the mass transport coefficient, c_j^e are the feed concentrations, and constants q_j^0 should be defined from the bulk problem. Thus the stationary concentration field c_j^s of Eq. (1) is defined by

$$D_j C_j q_j^0 (c_j^e - c_j^s)/p = - f_j(\theta(c_j^s)). \tag{2}$$

In order to study stability of the stationary solution, we consider small perturbations $\tilde{c}_j = c_j - c_j^s$. Linearizing Eq. (1) we obtain

$$\mathbf{W} \frac{\partial \tilde{\mathbf{c}}}{\partial t} = \mathbf{P} \frac{\partial \tilde{\mathbf{c}}}{\partial r} + \mathbf{A} \tilde{\mathbf{c}},$$

where $A_{jm} = (\partial f_j / \partial c_m)$ and W_{jm} are both computed at c_j^0.

We seek solutions of the perturbed problem in the form

$$\tilde{\mathbf{c}} = \sum_{k,n} \mathbf{s}_{(k,n)} e^{\lambda t + in\varphi + ikz},$$

where z, ϕ are the axial and angular coordinates and n should be an integer to ensure single valuedness. The eigenvalues λ dependent on k, n are obtained from the solvability conditions

$$\begin{gathered} |\mathbf{W}\lambda - \mathbf{PG} - \mathbf{A}| = 0, \\ \lambda^2 - \lambda \ \mathrm{tr}\ \mathbf{T}(k^2, n) + \det \mathbf{T}(k^2, n) = 0, \end{gathered} \tag{3}$$

where $\mathbf{T}(k^2, n) = \mathbf{W}^{-1}[\mathbf{A} + \mathbf{PG}(k^2, n)]$ and the transport operator represented by the diagonal matrix $\mathbf{G}_{jj} = q_j$ should be determined from the bulk problem. Two different kinds of instabilities are possible: a Turing instability across the flow with $n = 0$ and $k \neq 0$ (Secs. IV B and V B) and a DIFICI instability along the flow with $n \neq 0$ (Secs. IV C and V C).

III. SPECTRUM OF THE TRANSPORT OPERATOR

A. Convective diffusion equation

We compute the Fourier representation of the transport operator, which depends on the transport in the bulk flow and hence on the flow pattern. We consider convective diffusion in Couette flow between two coaxial cylinders with radii r_0 and r_1 ($r_0 < r_1$), as it is shown in Fig. 1. The outer cylinder rotates with the angular velocity ω, while the inner one is at rest and serves as a catalytic surface.

The flow is parallel and satisfies no-slip boundary conditions on the both cylinders. Thus only the angular velocity component differs from zero: $V_\varphi(r^*) = \omega r_1 (r^* - r_0)/(r_1 - r_0)$. Rescaling the coordinates by the gap between the cylinders $l = r_1 - r_0$ and introducing the dimensionless concentrations and rescaled parameters defined above we write the convective diffusion equation

$$\sigma \frac{\partial c_j}{\partial t} + \zeta r \frac{\partial c_j}{\partial \varphi} = d_j \Delta c_j ,$$

where Δ is the Laplace operator in cylindrical coordinates, $\zeta = (\omega l^2 / D_1)(r_1 / r_0)$ is a modified Péclet number, and the dimensionless parameter $\sigma = \kappa l^2 / (\gamma D_1)$ is the ratio of the diffusional and reaction time scales. We consider the *slow* reaction limit $\sigma \ll 1$ because all relevant effects become pronounced in this case. The concentration scales C_j will be specified later for specific reactions.

Since the species diffuse independently, we consider them separately and omit indices in this section. The transport equation is linear and the perturbation equation is the same; for $\sigma \rightarrow 0$ it is written as

$$\zeta r \frac{\partial \tilde{c}}{\partial \varphi} = d \Delta \tilde{c}.$$

We seek solutions of the form

$$\tilde{c} = e^{i(n\varphi + kz)} R(r),$$

where n is an integer. Restricting to the small gap limit $l \ll r_0$, we obtain the equation for $R(r)$

$$R'' - R(k^2 + inr\zeta)/d = 0. \tag{4}$$

This equation will be solved further with different boundary conditions on the outer cylinder to obtain the required transport operator.

B. Dirichlet boundary condition

First, we suppose that reactant is supplied from the outer cylinder, where the concentration is fixed: $c^*(r_1) = c^{*e}$. The condition for perturbation on the outer cylinder is

$$\tilde{c}(1) = 0. \tag{5}$$

Consider homogeneous perturbations that leave the surface homogeneous, i.e., do not depend on angular and axial coordinates $(k = n = 0)$. In this situation Eqs. (4) and (5) have a simple solution

$$R = (1 - r) R^0,$$

where the constant $R^0 = R(0)$ should be defined from the conditions on the catalytic surface. Thus the mass transport coefficient is $q^0 = -1$.

In the case $k \neq 0$ and $n = 0$ (which corresponds to Turing instability) Eq. (4) becomes

$$R'' - \delta^2 R = 0, \tag{6}$$

where $\delta = k d^{-1/2}$. The solution of Eq. (6) that satisfies the boundary conditions (5) is

$$R(r) = \frac{e^{\delta r} - e^{\delta(2-r)}}{1 - e^{2\delta}} R^0.$$

Thus, the spectral representation of the transport operator is

$$q(k,0) = R'(0) = -\delta \coth \delta.$$

The solution of Eq. (4) for $k = 0$ and $n \neq 0$ satisfying the boundary condition (5) is expressed through Airy functions

$$R(r) = R^0 3^{2/3} \Gamma(2/3) \, \frac{\mathrm{Bi}(\psi)\mathrm{Ai}(\psi r) - \mathrm{Ai}(\psi)\mathrm{Bi}(\psi r)}{\mathrm{Bi}(\psi) - \sqrt{3}\mathrm{Ai}(\psi)},$$

where

$$\psi = (in\zeta/d)^{1/3}. \tag{7}$$

This yields the spectral representation of the transport operator

$$q(0,n) = -s\psi \, \frac{\mathrm{Bi}(\psi) + \sqrt{3}\mathrm{Ai}(\psi)}{\mathrm{Bi}(\psi) - \sqrt{3}\mathrm{Ai}(\psi)}, \tag{8}$$

where

$$s = 3^{1/3} \frac{\Gamma\left(\frac{2}{3}\right)}{\Gamma\left(\frac{1}{3}\right)} \approx 0.729. \tag{9}$$

C. Neumann boundary condition

Alternatively, a Neumann (no-flux) boundary condition arises when there is no external supply of the chemical species. In the case $k = n = 0$, of course, $q(0,0) = 0$, but generally $q \neq 0$ at $k,n \neq 0$.

At $k \neq 0$, $n = 0$ we have

$$R(r) = \frac{e^{\delta r} + e^{\delta(2-r)}}{1 + e^{2\delta}} R^0.$$

Thus

$$q(k,0) = -k/\sqrt{d} \, \tanh(k/\sqrt{d}).$$

The solution of Eq. (4) for $k = 0$ and $n \neq 0$, satisfying the boundary condition (5), is again expressed through Airy functions

$$R(r) = R^0 3^{2/3} \Gamma(2/3) \, \frac{\mathrm{Bi}'(\psi)\mathrm{Ai}(\psi r) - \mathrm{Ai}'(\psi)\mathrm{Bi}(\psi r)}{\mathrm{Bi}'(\psi) - \sqrt{3}\mathrm{Ai}'(\psi)}$$

and

$$q(0,n) = -s\psi \, \frac{\mathrm{Bi}'(\psi) + \sqrt{3}\mathrm{Ai}'(\psi)}{\mathrm{Bi}'(\psi) - \sqrt{3}\mathrm{Ai}'(\psi)}, \tag{10}$$

where ψ, s are defined by Eqs. (7) and (9).

IV. BIMOLECULAR REACTION

A. Stationary states

As a first example, consider a bimolecular surface reaction of two species with the reaction rate expressions

$$f_j^* = -\kappa \theta_1 \theta_2, \quad j = 1,2,$$

and the Langmuir adsorption isotherm

$$\theta_j = \frac{b_j c_j^*}{1 + b_1 c_1^* + b_2 c_2^*}.$$

It is convenient to define the concentration scale C_j^* as the inverse capacitance factor of the jth reagent b_j. Then the surface reaction rate expressions become

$$f_j = -\frac{c_1 c_2}{(1 + c_1 + c_2)^2}.$$

For $c_2 > c_1 + 1$ or $c_2 < c_1 - 1$ one of the reactants is autocatalytic, so balance equations on the catalytic surface may have

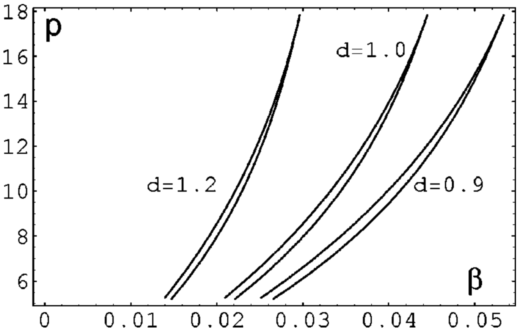

FIG. 2. Bimolecular reaction: bifurcation curves of stationary states in the parametric plane (β,p) for different values of d. Multiple stationary states exist within the cusped region.

multiple solutions. The solutions are spatially homogeneous since the stationary flux does not depend on transverse coordinates. The bifurcation conditions will be determined below.

Suppose that both reactants are supplied from the outer cylinder, i.e., the Dirichlet boundary conditions apply for both species. Consider homogeneous perturbations that leave the surface homogeneous, i.e., do not depend on angular and axial coordinates $(k=n=0)$. In this situation transport operators for both species are the same and $q_j(0,0)=-1$. The condition for bifurcation of stationary states $(\lambda=0)$ is

$$\det \mathbf{T}(0,0)=[c_2^0(1-c_1^0+c_2^0)d\beta+c_1^0(1+c_1^0-c_2^0) \\ +d\beta(1+c_1^0+c_2^0)^3/p]/p=0, \tag{11}$$

where $c_j^0 \equiv c_j^s(0)$ is the stationary concentration of j species at the catalytic surface, $\beta=b_1/b_2$, and $d=D_2/D_1$. After straightforward calculations, Eq. (11) together with Eq. (2) gives a family of cusped bifurcation loci in the (β,p) plane,

$$\beta(c_1^0)=\frac{c_1^e-c_1^0}{d\nu}, \\ p(c_1^0)=\frac{(1+c_1^0+c_2^e-\nu)^2(c_1^e-c_1^0)}{c_1^0(c_2^e-\nu)}, \tag{12}$$

where

$$\nu(c_1^0)=-\alpha_1\pm(\alpha_1^2-\alpha_0)^{1/2}, \\ \alpha_1(c_1^0)=[-(c_1^0)^2+c_1^0(1+c_1^e-c_2^e) \\ -c_1^e(1+2c_2^e)]/2(c_1^0+c_1^e), \tag{13} \\ \alpha_0(c_1^0)=c_2^e[2(c_1^0)^2-c_1^0c_1^e+c_1^e(1+c_2^e)]/(c_1^0+c_1^e),$$

and $0 \leqslant c_1^0 \leqslant c_1^e$ and $d>0$ are parameters. The bifurcation manifold shifts with the changing ratio of diffusion coefficients d of the two species, as shown in Fig. 2. Introducing d as an additional coordinate, we can draw the bifurcation manifold as a two-dimensional cusped surface in the parametric space (d,p,β). The bifurcation surface consists of two sheets joined at the cusp line. The boundaries of Turing instability and DIFICI domains are represented on both sheets as parametric curves. These curves divide the sheets into stable and unstable domains. The sheets are situated close to each other and have approximately the same qualitative picture of the instability domains. Thus we consider only one of the sheets. In the following, we shall look for bifurcations with spatial symmetry breaking on the lower sheet of the bifurcation surface, which is shown in Fig. 3.

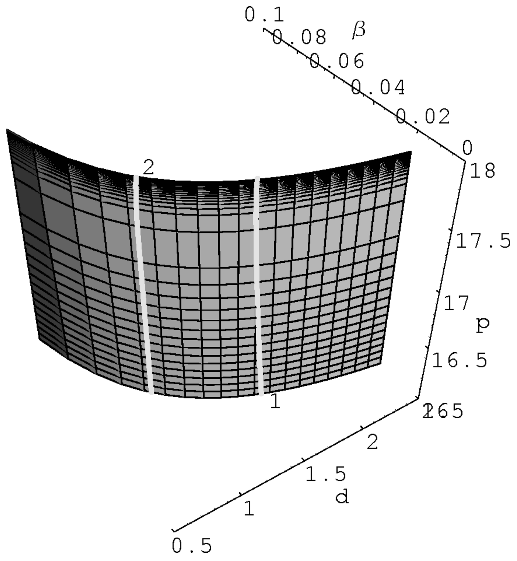

FIG. 3. Bimolecular reaction: boundaries of the Turing instability and DIFICI on the lower sheet of bifurcation surface. The Turing instability is observed to the left of the curve 1 and DIFICI to the right of the curve 2.

B. Turing instability

Turing instability is the result of axial perturbations with $k \neq 0$ (without angular perturbations, $n=0$). Thus the boundary of the Turing instability domain is defined by

$$\lambda(0,0)=0, \tag{14}$$

$$\frac{d\lambda}{d(k^2)}(0,0)=0. \tag{15}$$

The condition (14) is identical to the condition (11) and Eq. (12) can be considered as an additional condition on the parameter d. Thus, instead of the independent parameter d, one has to substitute the function obtained by solving Eq. (15) in Eqs. (12),

$$d(c_1^0)=1+\frac{(\xi_1+c_1^0)c_1^0}{(c_1^e-c_1^0)(\xi_1-c_1^0)},$$

where

$$\xi_1(c_1^0)=1+c_2^e-\nu(c_1^0) \tag{16}$$

and $\nu(c_1^0)$ is defined by Eq. (13). This defines the boundary of the Turing instability domain, shown by curve 1 in Fig. 3. The Turing instability domain lies to the left of this curve.

C. DIFICI

DIFICI results from growth of angular perturbations $(n \neq 0)$. In the continuous limit (valid for a cylinder with the circumference much larger than the gap width), the boundary of the DIFICI instability domain is defined by

$$\lambda(0,0)=0, \quad \frac{d\lambda_r}{d(n^2)}(0,0)=0. \tag{17}$$

As in the preceding subsection, the DIFICI domain is obtained from Eqs. (12) by replacing the parameter d by the following function obtained by resolving Eqs. (17):

$$d(c_1^0)=\frac{1}{2}[-\mathcal{K}_1\pm(\mathcal{K}_1^2-4\mathcal{K}_2\mathcal{K}_0)^{1/2}]\mathcal{K}_2^{-1},$$

where

$$\mathcal{K}_2(c_1^0)=\xi_2[-\xi_2(\xi_1+c_1^0)+\nu(1+c_1^0)\xi_3 + 17/35\nu\xi_3^2(c_1^e-c_1^0)],$$

$$\mathcal{K}_1(c_1^0)=\nu\xi_3[(1+c_1^0)(1-\xi_2)+\xi_2\xi_1(c_1^e-c_1^0) -\xi_3(c_1^e-c_1^0)]-2(\xi_1+c_1^0)\xi_2(1-\xi_2),$$

$$\mathcal{K}_0(c_1^0)=(1-\xi_2)[(\xi_2-1)(\xi_1+c_1^0) +\xi_1\xi_3(c_1^e-c_1^0)+17/35\nu(c_1^e-c_1^0)\xi_3^2],$$

$$\xi_2(c_1^0)=-\frac{(c_1^e-c_1^0)(\xi_1-c_1^0)}{c_1^0(\xi_1+c_1^0)}, \quad \xi_3(c_1^0)=\frac{c_1^0+c_2^e-\nu}{c_1^0(c_2^e-\nu)},$$

and $\nu(c_1^0)$ is defined by Eqs. (13) and $\xi_1(c_1^0)$ by Eq. (16). The boundary of the DIFICI domain is shown by curve 2 in Fig. 3. The DIFICI domain lies to the right of this curve. Thus, in the domain to the right of Turing curve there is no Turing instability, but there is the symmetry breaking caused by DIFICI.

V. BRUSSELATOR MODEL

A. Stationary solution and stability

As a second example of a surface reaction consider a version of the Brusselator model. It can be formulated as a system of two chemical reactions

$$A_1\underset{k_1}{\rightarrow}A_2, \quad 2A_1+A_2\underset{k_2}{\rightarrow}3A_1,$$

with the following reaction rates defined according to the mass action law:

$$R_{1,2}^*(\theta_1,\theta_2)=\pm\theta_1(k_1-k_2\theta_2\theta_1).$$

Taking k_1 as a reaction rate scale we obtain

$$f_{1,2}(\theta_1,\theta_2)=\pm\theta_1(1-\hat{\beta}\theta_2\theta_1),$$

where $\hat{\beta}=k_2/k_1$. Consider the Henry adsorption isotherm $\theta_j=H_jc_j$ as a relation between the surface coverages and bulk concentrations of both species near the surface. In this case $\mathbf{W}$ is the diagonal matrix with elements $W_{jj}=H_j$. Multiplying Eq. (1) by the inverse matrix $\mathbf{W}^{-1}$ from the left, we obtain

$$\frac{\partial c_1}{\partial t}=\frac{1}{p}\frac{\partial c_1}{\partial r}-c_1+\beta hc_2(c_1)^2,$$

$$\frac{\partial c_2}{\partial t}=\frac{d}{hp}\frac{\partial c_2}{\partial r}+\frac{1}{h}c_1-\beta c_2(c_1)^2,$$

where $h=H_2/H_1$, $\beta=\hat{\beta}H_1^2$, and $p=\hat{p}H_1$.

Suppose that one of the reactants is supplied from the outer cylinder (Dirichlet boundary condition), while there is no external input of the second one (Neumann boundary condition). In this case the transport operators for the two species will be different. The stationary homogeneous concentration field (2) is defined by

$$c_1^s=1, \quad c_2^s=1/(h\beta).$$

Consider the situation without perturbations along and around the inner cylinder, that is, $k=n=0$. In this case the components of the transport operator are $q_1=-1$ for the externally supplied species and $q_2=0$ for the species without external flux. Thus, in Eq. (3), we get

$$\begin{gathered}\lambda_r^2-\lambda_i^2-\lambda_r \operatorname{tr}\mathbf{T}+\det\mathbf{T}=0,\\ \lambda_i(2\lambda_r-\operatorname{tr}\mathbf{T})=0,\end{gathered} \tag{18}$$

where

$$\operatorname{tr}\mathbf{T}=1-\beta-1/p, \quad \det\mathbf{T}=\beta/p.$$

Since $\det\mathbf{T}$ is strictly positive, the homogeneous mode $\lambda=0$ is impossible. The Hopf bifurcation locus (p,β) is defined by the condition

$$1-\beta-1/p=0.$$

B. Turing instability

In this system both the Turing instability and DIFICI occur at nonzero values of k or n. At $n=0$ the components of the transport operator are $q_1(k)=-k\coth k$ and $q_2(k)=-k/\sqrt{d}\tanh(k/\sqrt{d})$; the matrix $\mathbf{T}$ is real and we have the same equations as Eqs. (18). However, now we have

$$\operatorname{tr}\mathbf{T}(k)=1-\beta-\frac{k}{hp}[h\coth k+\sqrt{d}\tanh(k/\sqrt{d})],$$

$$\det\mathbf{T}(k)=\frac{\beta k\coth k}{p}-\frac{\sqrt{d}}{hp}k\tanh\left(\frac{k}{\sqrt{d}}\right) +\frac{k^2\sqrt{d}}{hp^2}\coth k\tanh\left(\frac{k}{\sqrt{d}}\right).$$

An example of the dependence of the eigenvalues on k featuring a marginal Turing instability is shown in Fig. 4. Because of the absence of a homogeneous instability, there is no long-wavelength instability in this case, contrary to the first example. Now it is possible to have a short-wavelength instability, which requires stability for $k=0$ and instability for some $k=k^*\neq 0$. The stability conditions for $k=0$ are

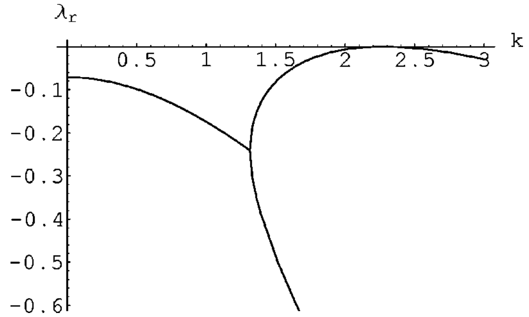

FIG. 4. Example of the dependence of the eigenvalues on k featuring marginal Turing instability.

$$\lambda_r^{(1)}(0)+\lambda_r^{(2)}(0)=\text{tr}\,\mathbf{T}(0)<0 \tag{19}$$

and

$$\lambda^{(1)}(0)\lambda^{(2)}(0)=\det\mathbf{T}(0)>0, \tag{20}$$

where the condition (20) is automatically satisfied because $\det\mathbf{T}(0)=\beta/p$ is obviously positive. If the condition (19) is true, i.e., $\text{tr}\,\mathbf{T}(0)<0$, then $\text{tr}\,\mathbf{T}(k)<0$ for all k because $\text{tr}\,\mathbf{T}(k)$ is a monotonically decreasing function. The Turing instability occurs if for some $k=k^*$ one of eigenvalues becomes equal to zero, that is,

$$\lambda^{(1)}(k^*)\lambda^{(2)}(k^*)=\det\mathbf{T}(k^*)=0. \tag{21}$$

We should add the condition that $\lambda^{(1)}(k^*)$ is the maximal value. Differentiating Eqs. (18) with respect to k at $k=k^*$ we obtain the conditions

$$\left(\frac{d}{dk}\det\mathbf{T}(k)\right)_{k^*}=0,\qquad \left(\frac{d^2}{dk^2}\det\mathbf{T}(k)\right)_{k^*}>0, \tag{22}$$

where $\det\mathbf{T}(k)$ can be rewritten as

$$\det\mathbf{T}(k)=Q\left\{\frac{h\beta}{\sqrt{d}}\coth\left(\frac{k}{\sqrt{d}}\right)-\tanh k+\frac{k}{p}\right\},$$

where $Q=(\sqrt{d}/hp)k\coth k\tanh(k/\sqrt{d})$ is positive for $k\neq 0$. For the following calculations Q can be omitted. Thus the conditions (19), (21), and (22) read

$$1-\beta-\frac{1}{p}<0, \tag{23}$$

$$\frac{h\beta}{\sqrt{d}}\coth\left(\frac{k^*}{\sqrt{d}}\right)-\tanh k^*+\frac{k^*}{p}=0, \tag{24}$$

$$-\frac{h\beta}{d}\,\frac{1}{\sinh^2(k^*/\sqrt{d})}-\frac{1}{\cosh^2 k^*}+\frac{1}{p}=0, \tag{25}$$

$$2\,\frac{h\beta}{d^{3/2}}\,\frac{\cosh(k^*/\sqrt{d})}{\sinh^3(k^*/\sqrt{d})}+2\,\frac{\sinh k^*}{\cosh^3 k^*}>0, \tag{26}$$

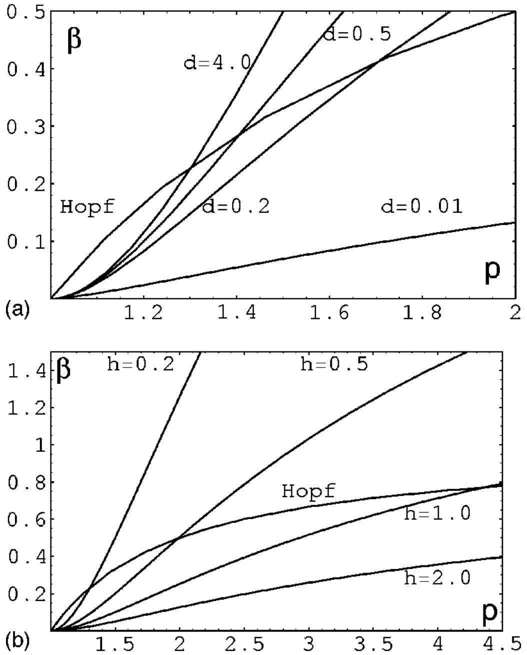

FIG. 5. Brusselator model: Turing instability for (a) $h=0.2$ and different values of d and (b) $d=4$ and different values of h. Instability occurs above the Hopf curve. The necessary instability condition is $h<\sqrt{d}$.

where condition (26) is always true $(k^*>0)$.

Equations (24) and (25) for all $h<\sqrt{d}$ can be rewritten as a parametric curve in the plane (p,β):

$$p(k)=\frac{\cosh^2 k[\sqrt{d}\sinh(2k/\sqrt{d})+2k]}{\sinh(2k)+\sqrt{d}\sinh(2k/\sqrt{d})},$$

$$\beta(k)=\frac{d}{h}\,\frac{\sinh^2(k/\sqrt{d})[\sinh(2k)-2k]}{\cosh^2 k[\sqrt{d}\sinh(2k/\sqrt{d})+2k]},$$

which should be considered for $\beta>(p-1)/p$ because of the condition (23). Turing instability curves for $h=0.2$ and different values of d from 0.01 up to 4.0 are shown in Fig. 5(a). Now the necessary condition $h<\sqrt{d}$ becomes obvious: The curve with $d=0.01$ ($h=0.2>\sqrt{d}=0.1$) always lies under the Hopf curve. Consequently, for increasing value of d the Turing instability occurs for smaller values of p and β. An analogous picture can be observed for $d=4$ and different values of h from 0.2 up to 2.0. Turing instability occurs on the parts of curves over the Hopf curve. For $h\geqslant 2$ there is no Turing instability. For a decreasing value of h we can observe Turing instability for smaller values of p and β, as it is shown in Fig. 5(b).

C. DIFICI

DIFICI is the result of angular perturbation with $n\neq 0$. Consider pure angular perturbations, i.e., with no axial perturbation. The transport operator is defined by Eq. (8) for the first species and by Eq. (10) for the second one. We are interested in obtaining a situation where instability occurs at some $n\neq 0$. The stability conditions for $n=0$ are

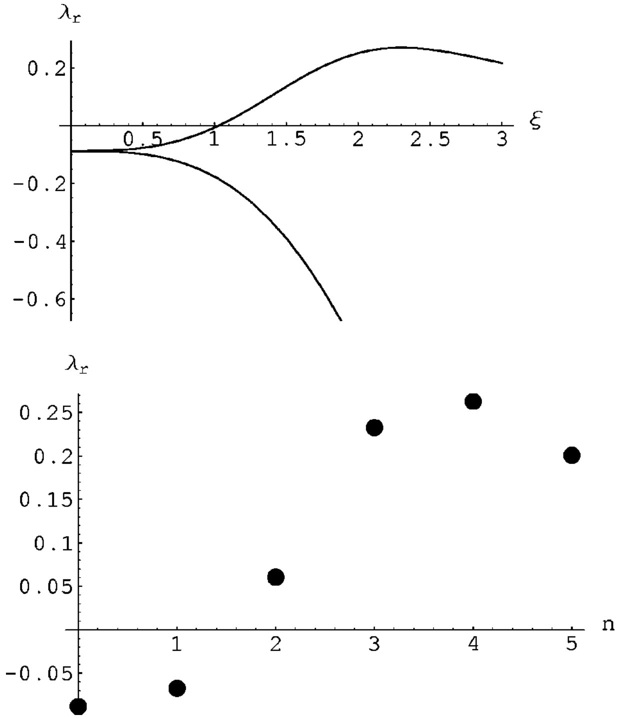

FIG. 6. Example of the dependence of the eigenvalues on *n* featuring DIFICI.

$$\lambda_r^{(1)}+\lambda_r^{(2)}=\mathrm{tr}_r\,\mathbf{T}<0, \tag{27}$$

$$\lambda^{(1)}\lambda^{(2)}=\det\mathbf{T}>0, \tag{28}$$

where $\det\mathbf{T}=\beta/p$, i.e., the condition (28) is automatically true. DIFICI may occur when for some n^* one of the eigenvalues becomes equal to zero, while the real part of the second one is negative. Thus, for $n=n^*$

$$\lambda_r^{(1)}+\lambda_r^{(2)}=\mathrm{tr}_r\,\mathbf{T}<0, \tag{29}$$

$$\lambda^{(1)}\lambda^{(2)}=\det\mathbf{T}=0. \tag{30}$$

The condition (29) may be excluded because the real part of tr **T** is a monotonically decreasing function of *n*. An example of the dependence of the eigenvalues on *n* is shown in Fig. 6.

The conditions (27) and (30) can be rewritten as a parametric curve in the plane (p,β),

$$p(\xi)=s\,\frac{\xi\phi_2^r(\xi)}{\phi_1^r(\xi)\phi_2^i(\xi)-\phi_1^i(\xi)\phi_2^r(\xi)},$$

$$\beta(\xi)=\frac{d^{2/3}}{h}\,\frac{\phi_1^r(\xi)}{\phi_2^r(\xi)},$$

where $\xi=(n\zeta)^{1/3}$ is the positive parameter and

$$\phi_j(\xi)=\left(\frac{\mathrm{I}_{-j/3}\left[\frac{2}{3}\sqrt{i\xi^3/d_j}\right]}{\mathrm{I}_{j/3}\left[\frac{2}{3}\sqrt{i\xi^3/d_j}\right]}\right)^{(-1)^j}, \quad j=1,2.$$

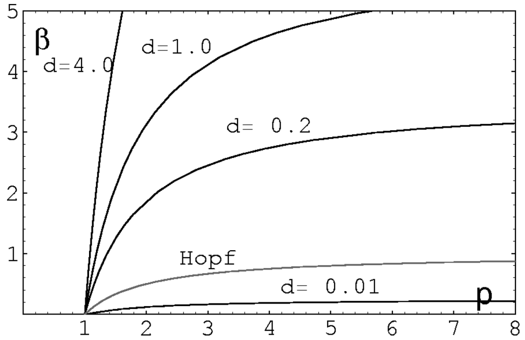

FIG. 7. Brusselator model: DIFICI curve for different values of *d*.

Here $\mathrm{I}_{\pm i/3}(t)$ are modified Bessel functions of fractional order. The results of calculation are shown in Figs. 7 and 8. The dependence of the DIFICI curve on different values of *h* is shown in Fig. 7. For smaller values of *h* instability occurs for smaller values of β and *p*, while the dependence of *d* is quite opposite: Over the specified value of *d* instability occurs for all values of β and $p>1$. For example, in case $d=6$ and $h=2$, DIFICI is possible for $p>1$ and $\beta>0$, while Turing instability is possible only for $p>p^*$, where $p^*\approx 26$ and $\beta>1$.

VI. CONCLUSION

The Couette flow reactor gives a unique opportunity to follow competition among DIFICI, Turing instability, and Hopf instability on an equiaccessible reaction surface. In both examples considered, a bimolecular catalytic reaction and the Brusselator model, we have obtained conditions for both kinds of symmetry-breaking instabilities, DIFICI and Turing instability, which fall into different parametric regions but may also interact at a higher codimension bifurcation locus.

A clear identification of various mechanisms of spontaneous symmetry breaking is possible only in a system possessing the involved symmetries to begin with, which may be difficult to realize experimentally. The original setup for DIFICI instability [2] was a one-dimensional reactor where translational symmetry was lacking from the outset, due to the existence of a preferred direction of the reactant supply that makes a uniform stationary state impossible for a generic (realistic) reaction system. This restriction also applies

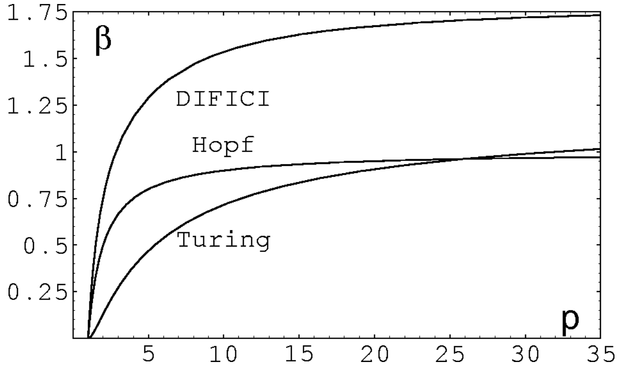

FIG. 8. Brusselator model: competition between Turing instability and DIFICI for $h=2$, $d=6$.

to the study of competition between the DIFICI in the direction of flow and a Turing instability in the transverse direction by Ponce Dawson *et al.* [6].

In the Couette flow reactor with diffusional supply of reactants analyzed in this paper, the symmetry of a uniform state may be broken by either DIFICI in the azimuthal or Turing instability in the axial direction. DIFICI is caused in this configuration by a disparity of adsorption rates of different reactants and is due essentially to a chromatographic effect. A more convenient way to supply reactants might be through axial flow. This, however, would break the symmetry along the axis. DIFICI in the azimuthal direction would still be possible in this configuration, but the state of broken symmetry would then branch off a spatially nonuniform basic state and DIFICI may be observed only in a part of the reactor.

We have given above a general recipe for the analysis of a surface reaction fed by diffusion and laminar advection. The procedure effectively separates the linear part of the problem by resolving the applicable partial differential equation in Fourier space and reducing the original three-dimensional problem to a closed two-dimensional evolution equation containing a nonlocal Dirichlet to Neumann operator. Once this operator is computed, the stability analysis of an arbitrary reaction scheme can be carried out in a standard way, although the actual computation of bifurcation loci may remain technically involved for rather trivial reasons, such as the necessity to solve cumbersome algebraic equations that possess multiple stationary states. In order to simplify algebra, full analysis has been carried out above for the artificial Brusselator system, while for a more realistic bimolecular system the existence of symmetry-breaking bifurcation was proved on the saddle-node bifurcation manifold. Although the wavelength of the bifurcating pattern is infinite on the intersection of the DIFICI or Turing instability and saddle-node bifurcation manifolds depicted in Fig. 3, the existence of broken-symmetry states with a large but finite wavelength in the vicinity of this intersection follows by continuity. This is supported by preliminary results of our numerical computations. The numerics is greatly facilitated by dimensional reduction with the help of a nonlocal operator. The computation of finite amplitude patterns based using the approach will be described elsewhere.

ACKNOWLEDGMENTS

L.M.P. acknowledges the support by the Fund for Promotion of Research at Technion. Y.B. acknowledges the support from the Technion–Israel Institute of Technology and the hospitality of Department of Computer Science, University of Wales.

[1] X.-G. Wu, S. Nakara, M. Menzinger, and A. Rovinsky, J. Phys. Chem. **100**, 158 (1996).
[2] A. B. Rovinsky and M. Menzinger, Phys. Rev. Lett. **69**, 1193 (1992).
[3] A. B. Rovinsky and M. Menzinger, Phys. Rev. Lett. **70**, 778 (1992).
[4] Y. Khazan and L. M. Pismen, Phys. Rev. Lett. **75**, 4318 (1995).
[5] J. D. Murray, *Mathematical Biology* (Springer-Verlag, Berlin, 1989).
[6] S. Ponce Dawson, A. Lawniczak, and R. Kapral, J. Chem. Phys. **100**, 5211 (1994).